

# DYNAMICS AND CONTROL OF THE REACTION MASS PENDULUM (RMP) AS A 3D MULTIBODY SYSTEM: APPLICATION TO HUMANOID MODELING

**Amit K. Sanyal**

Mechanical and Aerospace Engineering  
New Mexico State University  
Las Cruces, NM 88011  
Email: asanyal@nmsu.edu

**Ambarish Goswami**

Honda Research Institute US  
Mountain View, California 94043  
Email: agoswami@honda-ri.com

## ABSTRACT

Humans and humanoid robots are often modeled with different types of inverted pendulum models in order to simplify the dynamic analysis of gait, balance and fall. We have earlier introduced the Reaction Mass Pendulum (RMP), an extension of the traditional inverted pendulum models, which explicitly captures the variable rotational inertia and angular momentum of the human or humanoid. In this paper we present a thorough analysis of the RMP, which is treated as a 3D multibody system in its own right. We derive the complete kinematics and dynamics equations of the RMP system and obtain its equilibrium conditions. Next we present a nonlinear control scheme that stabilizes this underactuated system about an unstable set with a vertically upright configuration for the “leg” of the RMP. Finally we demonstrate the effectiveness of this controller in simulation.

## 1 Background and Motivation

Human and humanoid gait is often modeled with various versions of the inverted pendulum model, such as the 2D and 3D linear inverted pendulums (LIP) [1, 2], the cart-table model [3], the variable impedance LIP [4], the spring-loaded inverted pendulum [5], and the angular momentum pendulum model (AMPM) [6, 7]. These reduced models have been very beneficial for the analysis and prediction of gait and balance [8]. The inverted pendulum models allow us to ignore the movements of the multitude of individual limbs and instead focus on two points of fundamental importance – the center of mass (CoM) and the center of pressure (CoP) – and the “lean line” joining them.

A limitation of the above models (except [6, 7]) is that they represent the entire humanoid body only as a point mass and do not characterize the significant rotational inertia. Consequences of neglecting the rotational inertia is that the angular momentum of the system about its CoM,  $k_G$ , must be zero and the ground reaction force (GRF),  $f$  must be directed along the lean line. Humanoid robots, however, have no reason to obey these artificial

conditions, and in general, they do not. We have recently reported that during human gait, even at normal speed,  $f$  diverges from the lean line and this may be important for maintaining balance. Fig. 1 schematically depicts this important difference between the traditional inverted pendulum models and a planar model that contains non-zero rotational inertia.

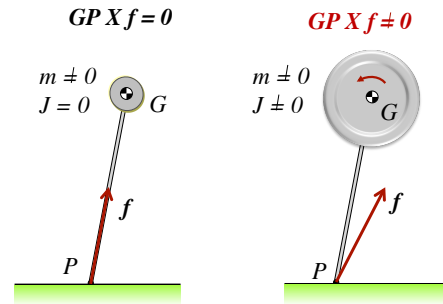


Figure 1. This figure illustrates the main difference between the traditional point-mass inverted pendulum model (left) and models containing non-zero rotational inertia (right). The point mass in the traditional pendulum model forces the ground reaction force,  $f$ , to pass through the center of mass. A reaction mass type pendulum, by virtue of its non-zero rotational inertia, allows the ground reaction force to deviate from the lean line. This has important implication in gait and balance.

The model with inertia captures the external centroidal moment (ECM),  $\tau_e$ , created by the GRF about the CoM and is given by  $\tau_e = GP \times f$ . Systems dynamics dictates that in the absence of external forces  $\tau_e = \dot{k}_G$ . The rotational inertia and the associated angular momentum are important components of humanoid movement and especially of balance, as have been re-

ported in [9]. Direct manipulation of angular and linear momentum has been suggested as a reasonable, and sometimes preferable, way to control a robot [10–12].

The Reaction Mass Pendulum (RMP) model [13] extends the existing inverted pendulum models by replacing the point mass at the top of the pendulum with an extended rigid body inertia. The linear mass of the system remains unchanged but the model now has a non-zero variable rotational inertia in the form of the 3D reaction mass which characterizes the *instantaneous* aggregate rotational inertia of the system projected at its CoM.

A humanoid controller based on a reduced model essentially attempts to impart to the humanoid the same dynamics as that of the reduced model. The differences between the robot dynamics, which is substantially more complex, and the dynamics of the reduced model is treated as an error and compensated by the controller. If the robot behavior is reasonably captured by the reduced model, the discrepancy between their dynamics is not dramatic, and the compensation is generally successful.

## 2 The RMP Model of a Humanoid

In this section we present a full description of the RMP model and explain how the model can be derived from a given humanoid. The RMP consists of two main parts: an actuated telescopic leg and an actuated body with a variable inertia. The leg makes a unilateral point contact with the ground and the friction is assumed sufficient to prevent its sliding. The body mass is attached at the CoM of the leg via a spherical “hip” joint, also considered fully actuated. The location of the hip joint coincides with the CoM of the body as well. The variable inertia of the body captures the centroidal composite rigid body (CCRB) inertia of the robot, which is the instantaneous generalized inertia of the entire robot projected at its CoM. The CCRB inertia is also called locked inertia in the field of geometric mechanics [14]. Additionally, the rotational motion of the body is such that the centroidal angular momentum of the RMP is instantaneously equal to that of the robot.

As a humanoid walks and moves through different limb configurations, its centroidal moment of inertia continuously changes. One way to capture this change is to imagine an ellipsoid corresponding to the positive definite inertia matrix of the robot. The changing shape, size and orientation of the ellipsoidal reaction mass will fully reflect the instantaneous inertia of the robot. This is depicted in Fig. 2. In the plane, the inertia ellipsoid becomes an inertia wheel [15] with continuously changing radius.

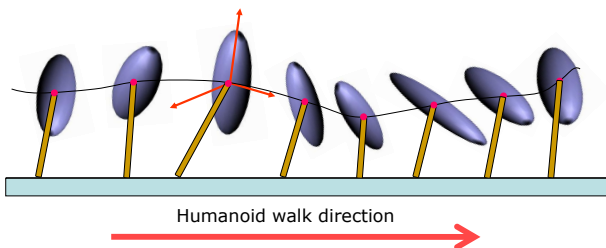


Figure 2. As the humanoid moves, its aggregate centroidal inertia continuously changes. At any instant, the aggregate inertia is reflected by the shape, size and orientation of the 3D reaction mass ellipsoid.

A mechanical model of a continuously changing inertia matrix is through the use of three pairs of point masses that are linearly actuated along three orthogonal directions. These directions coincide with the principal axes of the CCRB inertia ellipsoid. Along each axis, the pair of point masses move in synchrony such that they are always equidistant from the center; this makes the aggregate center of these masses fixed. The six point masses have equal mass, each having one-sixth of the total mass of the upper body of the humanoid. At a given instant the distances between the masses on each axis depend on the rotational inertia of the robot about that axis. This representation of the RMP is shown in Fig. 3 and is used as the basis for a novel multibody system as described in this paper in detail.

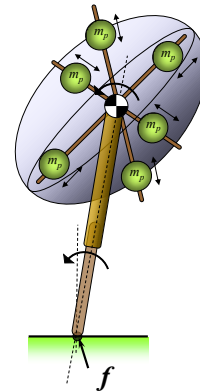


Figure 3. Conceptual mechanical realization of the 3D RMP. The RMP consists of a telescopic leg connecting the CoP and CoM, and a rotating body. In 3D, the rotating ellipsoidal body is mechanically equivalent to six equal masses on three mutually perpendicular rotating tracks. The CoM of the RMP is fixed at the common mid point of the tracks. This is the point about which the tracks themselves can rotate.

Note that we impose no direct condition on the kinetic energy of the RMP. As a consequence, the KE of the RMP and the humanoid, and therefore the scalar *Lagrangian* for the two systems, are not equal in general.

## 3 Dynamics of the Reaction Mass Pendulum

In this section, we give the mathematical model of the dynamics of the reaction mass pendulum.

### 3.1 Physical Configuration

The RMP model described in the earlier section is a multi-body system consisting of a variable-length leg and three pairs of proof mass actuators (PMAs) moving pairwise along three mutually orthogonal tracks. We refer to this assembly of tracks with proof mass actuators as the “PMA assembly” hereon in this paper. For simplicity in analysis, we consider the CoM of the leg of the RMP to always coincide with the CoM of the reaction mass ellipsoid. Therefore this also locates the CoM of the RMP system, which simplifies the dynamic analysis of the motion of the RMP. Motion of the RMP in 3D Euclidean space consists of: (1) translational motion of the CoM at the tip of the variable-length

leg; (2) rotational motion of the leg given by rotation and angular velocity of the leg about the CoM of the system; (3) rotational motion of the assembly of the PMAs about the CoM of the system; and (4) internal (shape) motion of the three pairs of PMAs along the three mutually orthogonal tracks.

### 3.2 Equations of Motion

Here we derive and provide the equations of motion of the RMP model, and obtain its equilibria.

**3.2.1 Kinematics and Configuration Space** We consider a body-fixed coordinate frame  $P$  for the RMP with its origin at the CoM and its axes aligned with the tracks of the PMAs, as shown in Fig. 4. We first define the configuration variables of the RMP as follows:

- $\rho \triangleq$  length of the leg of the RMP, which is also the distance between the CoM and the CoP,
- $R_L \triangleq$  rotation matrix from leg-fixed CoM frame to inertial frame fixed at CoP,
- $R_{PL} \triangleq$  rotation matrix from PMA assembly-fixed CoM frame to leg-fixed CoM frame,
- $s \triangleq [s_1 \ s_2 \ s_3]^T$  = vector of locations of the three pairs of proof mass actuators in the PMA assembly-fixed CoM frame.

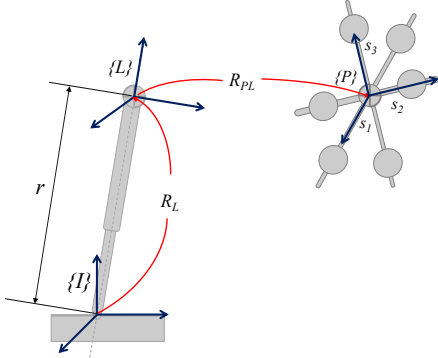


Figure 4. Three coordinate frames are used to describe the RMP kinematics: the CoP-fixed inertial frame  $I$ , the leg-fixed frame  $L$  located at the CoM and aligned with the leg axis, and the PMA assembly-fixed frame  $P$  located at the CoM.  $\rho$  is the length of the RMP leg,  $R_L$  is the rotation matrix from  $L$  to  $I$ ,  $R_{PL}$  is the rotation matrix from  $P$  to  $L$ , and  $s = [s_1 \ s_2 \ s_3]^T$  is the vector of locations of the three pairs of proof mass actuators in  $P$ .

Let the vector  $s$  be in a compact subspace  $\mathcal{S}$  of  $\mathbb{R}^3$  and the length  $\rho$  of the RMP leg be in a bounded interval  $[0, r]$  of  $\mathbb{R}$ . The configuration space of the RMP is therefore  $\mathcal{C} = [0, r] \times \text{SO}(3) \times \text{SO}(3) \times \mathcal{S}$ , which is ten dimensional, corresponding to the ten degrees of freedom (DOFs) of this RMP model. These DOFs are: one DOF corresponding to the scalar leg length  $\rho$ , three DOFs for the attitude of the leg  $R_L$ , three DOFs for the attitude of the PMA assembly  $R_{PL}$ , and three DOFs for the vector  $s$  of PMA locations. The inertial coordinate frame is defined such that its third axis is along the direction of the uniform gravity

force. Let  $e_i$  denote the  $i$ th column vector of the  $3 \times 3$  identity matrix. Therefore  $ge_3$  is the inertial acceleration vector due to uniform gravity, where  $g$  is the magnitude of this acceleration.

If the RMP leg-fixed coordinate frame has its third coordinate axis along the leg's longitudinal axis, the position of the CoM in the CoP-fixed inertial frame is  $b = \rho R_L e_3$ . Let the translational velocity of the CoM be represented by  $v$  in the leg-fixed CoM frame and let  $\Omega_L$  be the angular velocity about the CoM in the leg-fixed CoM frame. Let  $\Omega_{PL}$  denote the angular velocity of the PMA assembly with respect to the RMP leg. The kinematics for rotational motion of the leg about the CoM, rotational motion of the PMA assembly with respect to the RMP leg, and the translational motion of the CoM with respect to the CoP, are:

$$\dot{R}_L = R_L \Omega_L^\times \quad (1)$$

$$\dot{R}_{PL} = R_{PL} \Omega_{PL}^\times \quad (2)$$

$$v = R_L^T \dot{b} = \dot{\rho} e_3 + \rho \Omega_L \times e_3 \quad (3)$$

where  $\Omega^\times$  is the cross-product matrix defined by  $\Omega^\times v = \Omega \times v$ .

Therefore, the attitude of the PMA assembly with respect to the CoP-fixed inertial frame is  $R_P = R_L R_{PL}$ . The corresponding angular velocity of the PMA assembly with respect to the inertial frame is obtained from time derivative of  $R_P$  as

$$\dot{R}_P = R_P \Omega_P^\times \text{ where } \Omega_P = \Omega_{PL} + R_{PL}^T \Omega_L. \quad (4)$$

The position vectors of the  $i$ th pair of PMAs in the CoP-fixed inertial coordinate frame are  $b \pm R_P s_i e_i$ , for  $i = 1, 2, 3$ . The velocities of the proof masses in the  $i$ th proof mass pair are therefore:

$$v_{i+} = \dot{b} + R_P (\dot{s}_i e_i + \Omega_P \times e_i), \quad v_{i-} = \dot{b} - R_P (\dot{s}_i e_i + \Omega_P \times e_i),$$

where  $\dot{b} = R_L v$  is as given by equation (3).

**3.2.2 Dynamics of RMP** The dynamics of the three-dimensional RMP consists of the translational and rotational dynamics about its CoM and the dynamics of its internal states.  $\Gamma_L = R_L^T e_3$  denotes the direction of gravity expressed in the leg-fixed coordinate frame, since  $e_3 = [0 \ 0 \ 1]^T$  denotes the direction of gravity in the inertial frame. Let  $m_p$  denote the mass of each PMA (the six PMAs have equal masses) and let  $J_{P_0}$  denote the inertia tensor of the PMA frame minus the proof mass actuators about the CoM. Let  $m_L$  denote the mass and  $J_{L_0}$  denote the inertia tensor about the CoM of the leg of the RMP, so that the total mass of the RMP is  $m = 6m_p + m_L$ . The total kinetic energy of the PMA assembly is therefore given by

$$T_P = \sum_{i=1}^3 m_p (v^T v + \dot{s}_i^2) + \frac{1}{2} \Omega_P^T (J_{P_0} + K_P) \Omega_P, \quad (5)$$

where

$$K_P = -2 \sum_{i=1}^3 m_p s_i^2 (e_i^\times)^2 \text{ and } v^T v = \dot{\rho}^2 - \rho^2 \Omega_L^T (e_3^\times)^2 \Omega_L.$$

The kinetic energy of the RMP leg is given by

$$T_L = \frac{1}{2}m_L\dot{\rho}^2 + \Omega_L^T(J_{L_0} - m_L\rho^2(e_3^\times)^2)\Omega_L. \quad (6)$$

The total potential energy of the RMP system is given by

$$V = -mg\rho e_3^T R_L^T e_3 = -mg\rho e_3^T \Gamma_L. \quad (7)$$

Therefore the Lagrangian of the RMP is given by

$$\begin{aligned} \mathcal{L} &= T_P + T_L - V \\ &= \frac{1}{2}m\dot{\rho}^2 + \frac{1}{2}\Omega_L^T J_L \Omega_L + \frac{1}{2}\Omega_P^T J_P \Omega_P + m_p \dot{s}^T \dot{s} + mg\rho e_3^T \Gamma_L \end{aligned} \quad (8)$$

where  $K_L = -m\rho^2(e_3^\times)^2$ ,  $J_L = J_{L_0} + K_L$  and  $J_P = J_{P_0} + K_P$ .  $K_P$  and  $K_L$  are shape-dependent inertia terms.  $K_P$  accounts for the portion of the inertia of the PMA assembly that varies with  $s$ .  $K_L$ , on the other hand, varies with the leg length of the RMP.

In (8),  $\Omega_P$  is dependent on  $\Omega_L$ ,  $R_{PL}$  and  $\Omega_{PL}$  as given by (4). The following result gives the dynamics equations of motion for the RMP system.

**Proposition 1.** *Let  $f_L$  be the force applied by the prismatic actuator along the leg of the reaction mass pendulum in the inertial frame,  $\tau_P$  denote the control torque applied to the proof mass assembly resolved in its coordinate frame, and  $u_s$  be the vector of control forces applied to the proof mass actuators in the PMA-fixed coordinate frame. The dynamics of the reaction mass pendulum model are then given by the following equations*

$$m\ddot{\rho} = -m\rho\Omega_L^T(e_3^\times)^2\Omega_L + mge_3^T\Gamma_L + f_L, \quad (9)$$

$$\begin{aligned} J_L\dot{\Omega}_L &= J_L\Omega_L \times \Omega_L + 2m\rho\dot{\rho}(e_3^\times)^2\Omega_L + mg\rho e_3 \times \Gamma_L \\ &\quad - R_{PL}\tau_P, \end{aligned} \quad (10)$$

$$J_P\dot{\Omega}_P = J_P\Omega_P \times \Omega_P - N\Omega_P + \tau_P, \quad (11)$$

$$2m_p\dot{s} = L + u_s, \quad (12)$$

$$\text{where } N = \frac{d}{dt}K_P$$

$$= 4m_p \text{diag}\{s_2\dot{s}_2 + s_3\dot{s}_3, s_1\dot{s}_1 + s_3\dot{s}_3, s_1\dot{s}_1 + s_2\dot{s}_2\},$$

$$\text{and } L = \frac{\partial}{\partial s} \left( \frac{1}{2} \Omega_P^T K_P \Omega_P \right) = 2m_p \begin{bmatrix} s_1(\Omega_{P_2}^2 + \Omega_{P_3}^2) \\ s_2(\Omega_{P_3}^2 + \Omega_{P_1}^2) \\ s_3(\Omega_{P_1}^2 + \Omega_{P_2}^2) \end{bmatrix}.$$

The dynamics equations (9)-(12) are obtained by generalizing and applying the Lagrange-d'Alembert principle [16] to the non-linear configuration space  $\mathcal{C}$ . Variations of the state variables ( $R_L$  and  $R_{PL}$ ) in  $\text{SO}(3)$  are in the form of *reduced variations* [17, 18], as follows:

$$\delta R_L = R_L \Sigma_L^\times, \quad \delta R_{PL} = R_{PL} \Sigma_{PL}^\times, \quad (13)$$

where  $\Sigma_L, \Sigma_{PL} \in \mathbb{R}^3$  give variations along the manifold  $\text{SO}(3)$ . In addition, reduced variations of the angular velocities  $\Omega_L$  and  $\Omega_{PL}$  are given by [17, 18]:

$$\delta\Omega_L = \dot{\Sigma}_L + \Omega_L \times \Sigma_L, \quad \delta\Omega_{PL} = \dot{\Sigma}_{PL} + \Omega_{PL} \times \Sigma_{PL}, \quad (14)$$

where  $\dot{\Sigma}_L$  and  $\dot{\Sigma}_{PL}$  denote the time derivatives of  $\Sigma_L$  and  $\Sigma_{PL}$  respectively. The Lagrange-d'Alembert principle applied to the RMP system then takes the form

$$\int_{t_0}^{t_f} \left( \delta\mathcal{L} + \langle R_{PL}\tau_P^\times, \delta R_{PL} \rangle + f_L \delta\rho + u_s^T \delta s \right) dt = 0, \quad (15)$$

where  $\delta\mathcal{L}$  denotes the first variation of the Lagrangian  $\mathcal{L}$  with respect to all the state variables it depends on, and we define the inner product of two  $3 \times 3$  matrices by  $\langle A, B \rangle = \frac{1}{2} \text{trace}(A^T B)$ . Equation (15) holds for any time interval  $[t_0, t_f]$  over which the dynamics evolves. The equations of motion are then obtained from (15) by integration by parts and then evaluating the resulting equation for arbitrary fixed end-point variations  $\delta\rho$ ,  $\Sigma_L$ ,  $\Sigma_{PL}$  and  $\delta s$ . To save space on the presentation in this paper, we leave the complete derivation of equations (9)-(12) to the reader.

Note that these dynamics equations have the general form of the dynamics of an underactuated multibody system in uniform gravity, as given in [19]. Also note that equations (9)-(12) depend only on  $\Gamma = R_L^T e_3$  and not on the full attitude  $R_L$  of the leg. In other words, the equations of motion do not change if the inertial coordinate frame is rotated by an arbitrary angle about its z-axis, which represents the direction of uniform gravity. This is expected for a rigid body or multibody system in uniform gravity. We also note that the shape and attitude dynamics of the PMA assembly, given by equations (11)-(12) are directly coupled, and the attitude and shape (leg length) dynamic of the leg of the RMP, given by equations (9)-(10) are directly coupled. However, the only coupling between the dynamics of the RMP leg and that of the PMA assembly is through the torque  $\tau_P$  applied at the spherical joint connecting them. This is because the shape change of the PMA assembly is always "symmetric" about the center of mass, and therefore the CoM location is not varied by the symmetric movements of the three pairs of PMAs. This has important consequences in the design of control schemes for this system, as we show later.

**3.2.3 Equilibria of the RMP Dynamics** The conditions for equilibria of the RMP dynamics are obtained from the dynamics equations (9)-(12) and kinematics equations (1)-(3) by setting  $\dot{\rho} \equiv 0$ ,  $\Omega_L = \Omega_{PL} \equiv 0$ , and  $\dot{s} \equiv 0$ . This gives us:

$$\begin{aligned} mge_3^T \Gamma_L + f_L &= 0, \quad mg\rho e_3 \times \Gamma_L - R_{PL}\tau_P = 0, \quad \tau_P = 0, \\ \text{and } u_s &= 0. \end{aligned} \quad (16)$$

These conditions need to be simultaneously satisfied at an equilibrium of the RMP, which leads to  $\Gamma_L = \pm e_3$  and  $f_L = \mp mg$ , while the configuration variables ( $\rho, R_L, R_{PL}, s$ ) are constant at

the equilibria. Therefore, instead of disconnected (isolated) equilibrium points, we have two equilibrium manifolds for the RMP for which  $\Gamma_L = \pm e_3$  is along or opposite to the gravity direction, given by  $e_3$  in the inertial frame. These equilibrium manifolds are given by:

$$\mathcal{E}_1 = \{(\rho, R_L, R_{PL}, s, \dot{\rho}, \Omega_L, \Omega_{PL}, \dot{s}) \in TC : f_L = -mg, \Gamma_L = e_3, \dot{\rho} = 0, \Omega_L = \Omega_{PL} = 0, \dot{s} = 0\}, \quad (17)$$

$$\mathcal{E}_2 = \{(\rho, R_L, R_{PL}, s, \dot{\rho}, \Omega_L, \Omega_{PL}, \dot{s}) \in TC : f_L = mg, \Gamma_L = -e_3, \dot{\rho} = 0, \Omega_L = \Omega_{PL} = 0, \dot{s} = 0\}. \quad (18)$$

Since  $e_3$  denotes the direction of gravity in the inertial frame, we call  $\mathcal{E}_1$  the ‘‘hanging equilibrium manifold’’ and  $\mathcal{E}_2$  the ‘‘inverted equilibrium manifold’’. This terminology has been used in prior literature on rigid body and multibody pendulum models [20–23]. For modeling humanoid walking motion, the inverted equilibrium manifold of the RMP and its stabilization is of primary importance. We next look at a simplification of the reaction mass pendulum model with fixed proof masses.

### 3.3 RMP with Fixed Proof Masses

When the proof mass positions are fixed in the PMA body, the vector  $s$  is constant. This reduces the full dynamical model of the RMP, which has ten degrees of freedom (DOFs) as provided by equations (1)-(3) and (9)-(12), to one that has only seven degrees of freedom. The kinematic relations (1)-(3) still hold for this reduced model, since the DOFs associated with these relations ( $\rho$ ,  $\Omega_L$  and  $\Omega_{PL}$ ) are present in this reduced model. The configuration space of this reduced RMP system is  $\mathcal{P} = [0, r] \times \text{SO}(3) \times \text{SO}(3) \subset \mathcal{C}$ . Like the complete RMP model, this reduced model with fixed proof masses is also *underactuated*, with four actuated DOFs: one for the length of the RMP leg varied by the prismatic actuator, and the three rotational DOFs of the PMA assembly actuated by the torque applied at the spherical joint. The dynamics equations of motion are obtained by restricting  $s$  to be constant in the full dynamics model given by Proposition 1. This is stated below as Corollary 1.

**Corollary 1.** *The reduced reaction mass pendulum model depicted in Figure 3, with fixed proof mass positions in the proof mass assembly, has the following dynamics equations:*

$$m\ddot{\rho} = -m\rho\Omega_L^T(e_3^\times)^2\Omega_L + mge_3^T\Gamma_L + f_L, \quad (19)$$

$$J_L\dot{\Omega}_L = J_L\Omega_L \times \Omega_L + 2m\rho\dot{\rho}(e_3^\times)^2\Omega_L + mg\rho e_3 \times \Gamma_L - R_{PL}\tau_P, \quad (20)$$

$$J_P\dot{\Omega}_P = J_P\Omega_P \times \Omega_P + \tau_P, \quad (21)$$

$$\text{where } J_P = J_{P_0} - 2m_p \sum_{i=1}^3 s_i^2 (e_i^\times)^2. \quad (22)$$

Here  $s = [s_1 \ s_2 \ s_3]^T$  is the constant vector of positions of the proof masses in the coordinate frame fixed to the proof mass assembly.

## 4 Control of RMP

In this section, we present a control scheme for the underactuated reduced RMP model with fixed proof mass actuators presented in Section 3.3, to asymptotically stabilize a inverted leg attitude and length of the leg.

**Theorem 1.** *Consider the RMP system with fixed proof masses as given by equations (1)-(3) and equations (19)-(21). Let  $\Phi : \mathbb{R}^+ \rightarrow \mathbb{R}^+$  be a  $C^2$  function that satisfies  $\Phi(0) = 0$  and  $\Phi'(x) > 0$  for all  $x \in \mathbb{R}^+$ . Furthermore, let  $\Phi'(\cdot) \leq \alpha(\cdot)$  where  $\alpha(\cdot)$  is a Class- $\mathcal{K}$  function [24]. Let  $\gamma > 0$  and  $k > 0$  be positive scalar control gains,  $L$  be a  $3 \times 3$  positive definite gain matrix and let  $A = \text{diag}\{a_1, a_2, a_3\}$  where  $a_3 > a_2 > a_1 > 0$ . Let  $E_2 = \text{diag}\{-1, 1, -1\}$  be the desired final attitude of the leg of the RMP. Then the control laws*

$$f_L = -mge_3^T\Gamma_L - \gamma\dot{\rho} - k(\rho - \rho_e), \quad (23)$$

$$R_{PL}\tau_P = mg\rho e_3 \times \Gamma_L + L\Omega_L + \Phi'(\text{trace}(A - A_{Q_L}))S(Q_L), \quad (24)$$

$$\text{where } Q_L = E_2^T Q \text{ and } S(Q_L) = \sum_{i=1}^3 a_i Q_L^T e_i \times e_i,$$

asymptotically stabilize the set of motions defined by

$$\mathcal{S}_L = \{(\rho, R_L, R_{PL}, \dot{\rho}, \Omega_L, \Omega_{PL}) : \rho = \rho_e, R_L = E_2, \dot{\rho} = 0, \Omega_L = 0\}. \quad (25)$$

Moreover, the domain of stability of this set is almost global in the state space  $\mathcal{P} \times \mathbb{R}^7$ .

*Proof.* The proof of this result is obtained using generalizations of Lyapunov’s direct method and LaSalle’s invariance principle. The configuration space  $\mathcal{P}$  is a product set that has the compact, non-contractible manifold  $\text{SO}(3)$  as a factor. Moreover, the desired set we want to stabilize,  $\mathcal{S}_L$ , requires stabilization of the RMP leg attitude  $R_L \in \text{SO}(3)$  to a desired attitude given by  $R_L = E_2$ . Since any particular configuration on  $\text{SO}(3)$ , which is the configuration space for rigid body attitude, cannot be globally asymptotically stabilized using continuous feedback (see [25–28]), we obtain almost global stabilization of the desired set  $\mathcal{S}_L$ . Moreover, for continuous stabilization of the leg attitude, we need a Morse function that generalizes the concept of a Lyapunov function to a nonlinear space [29]. The candidate Morse-Lyapunov function  $V : \mathcal{P} \times \mathbb{R}^7 \rightarrow \mathbb{R}^+$  for stabilizing the motion of the leg is defined by

$$V(\rho, R_L, \dot{\rho}, \Omega_L) = \frac{1}{2}m\dot{\rho}^2 + \frac{1}{2}\Omega_L^T J_L \Omega_L + \frac{1}{2}k(\rho - \rho_e)^2 + \Phi(\text{trace}(A - A_{Q_L})). \quad (26)$$

The time derivative of this Lyapunov function is given by

$$\dot{V} = m\dot{\rho}\ddot{\rho} + \Omega_L^T J_L \dot{\Omega}_L - m\rho\dot{\rho}\Omega_L^T(e_3^\times)^2\Omega_L + k(\rho - \rho_e)\dot{\rho} + \Phi'(\text{trace}(A - A_{Q_L}))\Omega_L^T S(Q_L),$$

where the last term is the time derivative of  $\Phi(\text{trace}(A - AQ_L))$  and  $\Phi'(x)$  denotes the derivative of  $\Phi(x)$  with respect to  $x$ . Substituting the dynamics equations (19)-(20) into the above expression for  $\dot{V}$ , we get

$$\dot{V} = \dot{\rho} [mge_3^T \Gamma_L + f_L + k(\rho - \rho_e)] + \Omega_L^T [mg\rho e_3 \times \Gamma_L + \Phi'(\text{trace}(A - AQ_L))S(Q_L) - R_{PL}\tau_P]$$

Further substitution of the control laws (23)-(24) into this last expression for  $\dot{V}$  gives us

$$\dot{V} = -\gamma\dot{\rho}^2 - \Omega_L^T L \Omega_L, \quad (27)$$

hence the time derivative of this Morse-Lyapunov function is negative semidefinite for the closed-loop system given by equations (1)-(3) and (19)-(21), and the control laws (23)-(24). Therefore the feedback system is Lyapunov stable at the set  $S_L$ .

To show asymptotic stability, we first consider the set of motions for which  $\dot{V} \equiv 0$ ; which is equivalent to both  $\dot{\rho} \equiv 0$  and  $\Omega_L \equiv 0$ . When we substitute these in the dynamics equations (19)-(20) for the RMP leg, we get

$$mge_3^T \Gamma_L + f_L = 0 \text{ and } mg\rho e_3 \times \Gamma_L - R_{PL}\tau_P = 0, \quad (28)$$

where  $f_L$  and  $\tau_P$  are obtained from the control laws (23)-(24). Substituting  $\dot{\rho} \equiv 0$  and  $\Omega_L \equiv 0$  into these feedback control laws and the expressions in (28), we get

$$-k(\rho - \rho_e) = 0 \text{ and } -\Phi'(\text{trace}(A - AQ_L))S(Q_L) = 0, \quad (29)$$

which characterizes the largest invariant set  $\mathbf{I} \subset \dot{V}^{-1}(0) \subset \mathcal{P} \times \mathbb{R}^7$ . As shown in [26], the set of critical points of  $\Phi(\text{trace}(A - AQ_L)) : \text{SO}(3) \rightarrow \mathbb{R}^+$  is

$$Q_L \in \mathcal{E}_c \triangleq \{I, \text{diag}\{-1, 1, -1\}, \text{diag}\{1, -1, -1\}, \text{diag}\{-1, -1, 1\}\} \subset \text{SO}(3). \quad (30)$$

Therefore, the set  $\mathbf{I}$  is defined by

$$\mathbf{I} = \left\{ (\rho, R_L, R_{PL}, \dot{\rho}, \Omega_L, \Omega_{PL}) : \rho = \rho_e, Q_L = E_2^T R_L \in \mathcal{E}_c, \dot{\rho} = 0, \Omega_L = 0 \right\}. \quad (31)$$

Hence, according to LaSalle's invariance principle [24], all solutions of the feedback system given by (1)-(3), (19)-(21), and the control laws (23)-(24) converge to the set  $\mathbf{I} \subset \mathcal{P} \times \mathbb{R}^7$ . Within the set of critical points  $\mathcal{E}_c$  of  $\Phi(\text{trace}(A - AQ_L))$ , it has been shown [26-28] that  $Q_L = I$  is the minimum, while the other points ( $Q_L \in \mathcal{E}_c \setminus I$ ) are non-degenerate critical points. Therefore, as  $\dot{V} \leq 0$  along the trajectories of the feedback system, the

only stable subset of the invariant set is  $S_L \subset \mathbf{I}$ . The other subsets (corresponding to  $Q_L \in \mathcal{E}_c \setminus I$ ) are unstable, although they may have stable subsets. Hence, except for those trajectories that start on the stable subsets of  $\mathbf{I} \setminus S_L$ , all other trajectories in  $\mathcal{P} \times \mathbb{R}^7$  converge asymptotically to the set  $S_L$ . Since the largest invariant set  $\mathbf{I}$  of the feedback system is itself of zero measure in the state space  $\mathcal{P} \times \mathbb{R}^7$ , this means that the set  $S_L$  is asymptotically stable and its domain of attraction is almost global.  $\square$

Note that the control scheme given by Theorem 1 only stabilizes an upright attitude and fixed length of the RMP leg; it does not stabilize the motion of the PMA assembly to an equilibrium position and attitude. However, stabilizing the inverted leg attitude with desired leg length is a first step in obtaining more general control schemes that could stabilize an inverted equilibrium configuration of the RMP.

## 5 Simulation and Discussion

In this section, we present a numerical simulation for the feedback RMP system given by equations (1)-(3), (19)-(21), and the control laws (23)-(24). The initial conditions for the configuration variables in the system are given by:

$$R_L(0) = \begin{bmatrix} 0.8753 & 0.2918 & 0.3857 \\ -0.4136 & 0.8650 & 0.2842 \\ -0.2507 & -0.4082 & 0.8778 \end{bmatrix}, \quad \rho(0) = 0.8322 \text{ m},$$

$$R_{PL}(0) = \begin{bmatrix} 0.6882 & -0.6572 & -0.3073 \\ 0.3456 & 0.6694 & -0.6576 \\ 0.6379 & 0.3464 & 0.6878 \end{bmatrix}.$$

The initial leg attitude  $R_L(0)$  makes an angle of  $151.37^\circ$  to the direction of uniform gravity (inertial z-axis), while the initial attitude of the PMA assembly is obtained by a rotation of an angle of  $22.5^\circ = \frac{\pi}{8}$  radians about the axis  $[1 \ -1 \ 1]^T / \sqrt{3}$  in the leg-fixed coordinate axis. The initial velocities are set to zero, i.e.,  $\Omega_L = [0 \ 0 \ 0]^T$  rad/s,  $\dot{\rho} = 0$  m/s, and  $\Omega_{PL} = [0 \ 0 \ 0]^T$  m/s. The mass and inertia properties for this simulation are:

$$m_L = 1.26 \text{ kg}, \quad J_{L_0} = \text{diag}\{0.98, 0.91, 0.63\} \text{ kg-m}^2,$$

$$m_P = 0.33 \text{ kg}, \quad J_{P_0} = \text{diag}\{0.21, 0.21, 0.21\} \text{ kg-m}^2.$$

The vector of constant positions for the three pairs of proof masses is given by

$$s = [0.21 \ 0.21 \ 0.21]^T \text{ m}.$$

The desired set of motions to be stabilized is given by  $S_L$  in equation (25) with  $\rho_e = 0.7$  m. We numerically simulate the dynamics of the feedback system over a period of 70 seconds. Figure 5 gives the time plot of  $\Delta\rho = \rho - \rho_e$  for the feedback system. Figure 6 gives the time plot of the angle  $\Phi$  between the  $\Gamma_L$  vector and the direction of uniform gravity, i.e.,  $\cos\Phi = e_3^T \Gamma_L = e_3^T R_L^T e_3$ . In [20-23, 25],  $\Gamma_L$  is referred to as the *reduced attitude* vector of the rigid or multibody pendulum system. Both the configuration variables  $\rho$  and  $\Gamma_L$  are seen to converge to the desired final values during the time period of this simulation. Figure 7 gives the time evolution of the velocity vari-

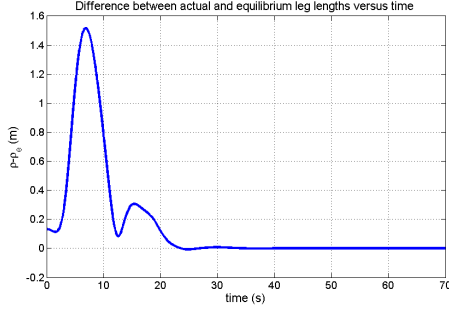


Figure 5. Time plot of  $\rho - \rho_e$  for the reduced RMP system with the feedback control scheme of Theorem 1. Here  $\rho_e = 0.7$  m and the initial value of  $\rho$  is 0.8322 m.

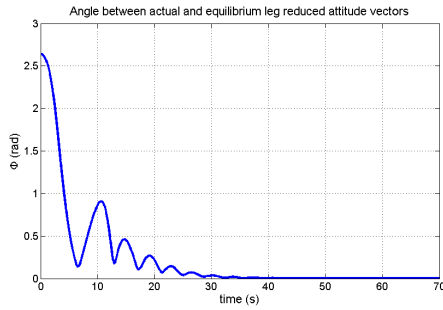


Figure 6. Time plot of the angle  $\Phi$  between the reduced attitude  $\Gamma_L$  of the RMP leg and the direction of uniform gravity, for the reduced RMP system with the feedback control scheme of Theorem 1. Here  $\Phi = 151.37^\circ$  at the start of the simulation and the final desired value of  $\Phi$  is  $0^\circ$ .

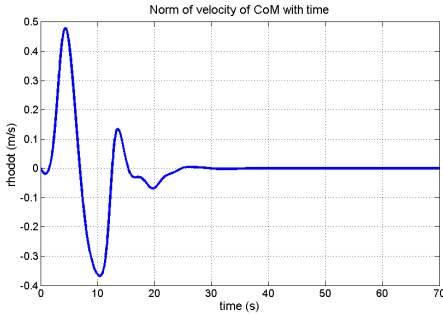


Figure 7. Time plot of the velocity  $\dot{\rho}$  of extension or retraction of the RMP leg, for the reduced RMP system with the feedback control scheme of Theorem 1. Both the initial and the final desired value of  $\dot{\rho}$  is 0 m/s.

able  $\dot{\rho}$ , which is the speed of extension or retraction of the leg of the RMP by the prismatic actuator. Figure 8 gives the time plots of the components of the angular velocity vector  $\Omega_L$  of the RMP leg over the simulation period. It is to be noted that these velocity states are seen asymptotically converge to zero over the time period of simulation (70 s). Finally, we give the time plot of the angular velocity  $\Omega_P$  of the PMA assembly during this simulation period, in Figure 9. Note that the PMA assembly is in torque-free rigid body rotational motion when the leg dynamics is restricted to the stable set  $\mathcal{S}_L$ .

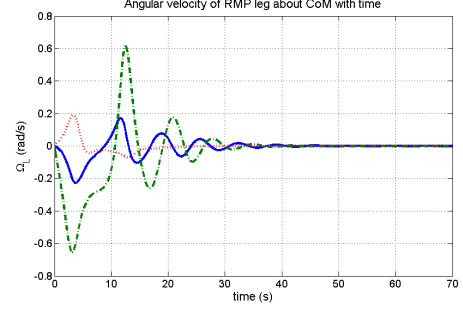


Figure 8. Time plots of the components of the angular velocity  $\Omega_L$  of the RMP leg, for the reduced RMP system with the feedback control scheme of Theorem 1. Both the initial and the final desired values of these components are 0 rad/s.

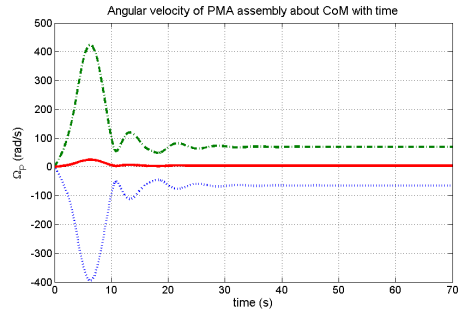


Figure 9. Time plots of the components of the angular velocity  $\Omega_P$  of the RMP PMA assembly, for the reduced RMP system with the feedback control scheme of Theorem 1.

## 6 Conclusions and Future Work

We have introduced the reaction mass pendulum (RMP) as a multibody, reduced order model of a humanoid robot. It is an instantaneous capture of the 3D aggregate kinematics and inertia of a humanoid robot, consisting of a variable length leg and a proof mass assembly with three pairs of proof masses. The reaction mass pendulum model is an enhancement of existing inverted pendulum humanoid models that contain only a point mass, and is also a mechanical realization of variable rotational inertia that characterizes the humanoid and accounts for the presence of centroidal angular momentum. In this work, we derived the dynamics equations of motion using a global representation of the state of this multibody RMP model. We also obtained a control scheme that asymptotically stabilizes an inverted “upright” configuration of the leg of the RMP. The domain of attraction of this control scheme is shown to be almost global in the state space. In the future, we plan to extend this work to stabilization of an inverted equilibrium configuration for both the leg and the proof mass assembly of the RMP.

## ACKNOWLEDGMENT

AKS has benefitted from discussions and collaborative work with Harris McClamroch and Nalin Chaturvedi on 3D pendulum systems. AG is grateful to Ken Waldron for his early help with the 3D RMP equations, and Sun-Hee Lee for help in developing

the RMP model.

## REFERENCES

- [1] Kajita, S., and Tani, K., 1991. "Study of dynamic biped locomotion on rugged terrain". In IEEE International Conference on Robotics and Automation (ICRA), pp. 1405–1411.
- [2] Kajita, S., Kanehiro, F., Kaneko, K., Yokoi, K., and Hirukawa, H., 2001, Maui, Hawaii. "The 3D linear inverted pendulum mode: A simple modeling for a biped walking pattern generator". In IEEE/RSJ International Conference on Intelligent Robots and Systems (IROS), pp. 239–246.
- [3] Kajita, S., Kanehiro, F., Kaneko, K., Fujiwara, K., Harada, K., Yokoi, K., and Hirukawa, H., 2003, Taipei, Taiwan. "Biped walking pattern generation by using preview control of zero-moment point". In IEEE International Conference on Robotics and Automation (ICRA), pp. 1620–1626.
- [4] Sugihara, T., and Nakamura, Y., 2003, Germany. "Variable impedant inverted pendulum model control for a seamless contact phase transition on humanoid robot". In IEEE International Conference on Humanoid Robots (Humanoids2003).
- [5] Altendorfer, R., Saranlı, U., Komsuoglu, H., Koditschek, D., Brown, H. B., Buehler, M., Moore, N., McMordie, D., and Full, R., 2001. "Evidence for spring loaded inverted pendulum running in a hexapod robot". In *Experimental Robotics VII*, D. Rus and S. Singh, eds. Springer-Verlag, pp. 291 – 302.
- [6] Komura, T., Leung, H., Kudoh, S., and Kuffner, J., 2005, Barcelona, Spain. "A feedback controller for biped humanoids that can counteract large perturbations during gait". In IEEE International Conference on Robotics and Automation (ICRA), pp. 2001–2007.
- [7] Komura, T., Nagano, A., Leung, H., and Shinagawa, Y., 2005, September. "Simulating pathological gait using the enhanced linear inverted pendulum model". *IEEE Transactions on Biomedical Engineering*, **52**(9), pp. 1502–1513.
- [8] Kuo, A., 2007. "The six determinants of gait and the inverted pendulum analogy: A dynamic walking perspective". *Human Movement Science*, **26**(4), pp. 617–656.
- [9] Herr, H., and Popovic, M., 2008. "Angular momentum in human walking". *The Journal of Experimental Biology*, **211**, pp. 467–481.
- [10] Hofmann, A., 2006. "Robust execution of biped walking tasks from biomechanical principles". PhD thesis, MIT, AI Lab.
- [11] Kajita, S., Kanehiro, F., Kaneko, K., Fujiwara, K., Harada, K., Yokoi, K., and Hirukawa, H., 2003, Las Vegas, NV, USA. "Resolved momentum control: humanoid motion planning based on the linear and angular momentum". In IEEE/RSJ International Conference on Intelligent Robots and Systems (IROS), Vol. 2, pp. 1644–1650.
- [12] Vermeulen, J., Verrelst, B., Vanderborght, B., Lefeber, D., and Guillaume, P., 2006. "Trajectory planning for the walking biped lucy". *International Journal of Robotics Research*, **25**(9), pp. 867–887.
- [13] Lee, S.-H., and Goswami, A., 2007. "Reaction mass pendulum (RMP): An explicit model for centroidal angular momentum of humanoid robots". In IEEE International Conference on Robotics and Automation (ICRA), pp. 4667–4672.
- [14] Hernandez-Garduno, A., Lawson, J. L., and Marsden, J. E., 2004. Relative equilibria for the generalized rigid body. Tech. rep., Mathematics Faculty Research Paper. Trinity University.
- [15] Block, D., Astrom, K.J., and Spong, M., 2007. *The Reaction Wheel Pendulum*. Morgan and Claypool Publishers.
- [16] Goldstein, H., 1980. *Classical Mechanics*, 2 ed. Addison-Wesley, Reading, MA.
- [17] Bloch, A. M., 2003. *Nonholonomic Mechanics and Control*. No. 24 in Interdisciplinary Texts in Mathematics. Springer Verlag.
- [18] Abraham, R., and Marsden, J. E., 1978. *Foundations of Mechanics*, 2 ed. Benjamin/Cummings Publishing Company.
- [19] Shen, J., 2002. "Nonlinear control of multibody systems with symmetries via shape change". PhD thesis, University of Michigan, Ann Arbor, MI, July.
- [20] Shen, J., Sanyal, A. K., Chaturvedi, N. A., Bernstein, D. S., and McClamroch, N. H., 2004, Nassau, Bahamas. "Dynamics and control of a 3D pendulum". In IEEE Conference on Decision and Control, pp. 323–328.
- [21] Shen, J., Sanyal, A. K., and McClamroch, N. H., 2003. "Asymptotic stability of multibody attitude systems". In *Stability and Control of Dynamical Systems with Applications*, D. Liu and J. Antsaklis, eds. Birkhauser, pp. 291–302.
- [22] Chaturvedi, N. A., Bacconi, F., Sanyal, A. K., Bernstein, D. S., and McClamroch, N. H., 2005, Portland, Oregon. "Stabilization of a 3D rigid pendulum". In American Control Conference, pp. 3030–3035.
- [23] Chaturvedi, N. A., and McClamroch, N. H., 2006, San Diego, CA. "Global stabilization of an inverted 3D pendulum including control saturation effects". In IEEE Conference on Decision and Control, pp. 6488–6493.
- [24] Khalil, H. K., 1995. *Nonlinear Systems*, 2 ed. Prentice Hall, Englewood Cliffs, NJ.
- [25] Chaturvedi, N. A., McClamroch, N. H., and Bernstein, D. S., 2009. "Asymptotic smooth stabilization of the inverted 3d pendulum". *IEEE Transactions on Automatic Control*, **54**(6), June, pp. 1204–1215.
- [26] Sanyal, A. K., and Chaturvedi, N. A., 2008, Honolulu. "Almost global robust attitude tracking control of spacecraft in gravity". In AIAA Guidance, Navigation and Control Conference, pp. AIAA–2008–6979.
- [27] Sanyal, A. K., Fosbury, A., Chaturvedi, N. A., and Bernstein, D. S., 2009. "Inertia-free spacecraft attitude trajectory tracking with disturbance rejection and almost global stabilization". *AIAA Journal of Guidance, Control and Dynamics*, **32**(2), Feb, pp. 1167–1178.
- [28] Chaturvedi, N. A., Sanyal, A. K., and McClamroch, N. H., 2011. "Rigid-Body Attitude Control: Using rotation matrices for continuous, singularity-free control laws". *IEEE Control Systems Magazine*, **31**(6), June, p. to appear.
- [29] Milnor, J., 1963. *Morse Theory*. Princeton University Press, Princeton, NJ.